applied sciences

MDPI

Article

The Effect of Surface-Coating Materials on the Flexural Properties and Surface Integrity of a 3D-Printed Denture Base Resin: An In Vitro Study

Ioannis Tsolianos [1], Olga Naka [1], Savvas Kamalakidis [1,2], Stavros Chatzopoulos [3], Apostolos Argyros [4,5], Nikolaos Michailidis [4,5] and Eleni Kotsiomiti [1,*]

[1] Department of Prosthodontics, School of Dentistry, Faculty of Health Sciences, Aristotle University of Thessaloniki, 54124 Thessaloniki, Greece; itsolia@dent.auth.gr (I.T.); naka@dent.auth.gr (O.N.); drkamalakidis@dent.auth.gr (S.K.)
[2] Department of Prosthodontics, School of Dental Medicine, Tufts University, Boston, MA 02111, USA
[3] Department of Statistics, University of Western Macedonia, 51100 Grevena, Greece; schatzopoulos@uowm.gr
[4] Physical Metallurgy Laboratory, Mechanical Engineering Department, School of Engineering, Aristotle University of Thessaloniki, 54124 Thessaloniki, Greece; aargyros@auth.gr (A.A.); nmichail@auth.gr (N.M.)
[5] Centre for Research & Development of Advanced Materials (CERDAM), Aristotle University of Thessaloniki and Texas A&M Engineering Experiment Station, Centre for Interdisciplinary Research and Innovation, 57001 Thessaloniki, Greece
* Correspondence: kotsiom@dent.auth.gr

Abstract

3D-printed denture base resins offer significant workflow advantages in denture fabrication, but may exhibit limitations in mechanical performance and surface quality. This in vitro study evaluated the effects of different surface-coating materials on the flexural properties and surface integrity of a 3D-printed denture base resin. Stereolithography-fabricated specimens were airborne-particle abraded and coated with single or double layers of four commercial glaze materials and an unpolymerized denture base resin; untreated specimens served as controls. Flexural properties were assessed utilizing an ISO 20795-1-based design, and surface morphology was evaluated using scanning electron microscopy (SEM) after 90 days of water immersion. Coating application (single versus double layers) did not significantly influence flexural strength or modulus. The control group exhibited the highest mean flexural strength. The unpolymerized resin groups performed closely to the ISO benchmark, whereas commercial coatings failed to enhance mechanical properties, occasionally reducing them below this reference value. Morphological analysis revealed surface irregularities in coatings lacking nanoparticles, whereas nanoparticle-containing coatings showed no visible surface defects after water storage. In conclusion, commercial glazes should be used with caution on 3D-printed resins due to potential mechanical compromise. The application of nanoparticle-containing coatings resulted in a stable surface topography, and unpolymerized resin coatings emerged as a feasible alternative.

Keywords: 3D-printing; denture base; flexural properties; glazing; surface integrity

Check for updates

Academic Editor: Amaury Pozos-Guillen

Received: 30 September 2026
Revised: 21 October 2026
Accepted: 27 October 2026
Published: 28 October 2026

Copyright: © 2026 by the authors. Licensee MDPI, Basel, Switzerland. This article is an open access article distributed under the terms and conditions of the Creative Commons Attribution (CC BY) license.

1. Introduction

Complete dentures are subjected to complex mechanical stresses on a daily basis, especially during mastication, which cause repetitive bending stresses of the acrylic resin material [1,2]. Inadequate bending strength can lead to fractures and compromise long-term clinical performance [3,4]. Flexural strength and flexural modulus are critical mechanical properties of denture base materials, as they determine the ability of the prosthesis to

withstand functional loads without permanent deformation or fracture [5,6]. Therefore, optimizing the flexural properties of denture base materials remains a primary goal in contemporary removable prosthodontics.

The integration of digital 3D printing technologies has transformed denture fabrication, offering reduced production time, lower costs, and fewer clinical visits compared to conventional protocols [7–9] or subtractive milling techniques [10,11]. Concurrently, advancements in photopolymerizable resins have broadened the clinical applications of 3D printing [12]. However, 3D-printed denture base resins often exhibit inferior mechanical properties, such as reduced flexural strength and lower fracture toughness, than conventional and CAD-CAM milled resins [10,13]. This drawback has been attributed to the photopolymerization process, degree of monomer conversion, resin composition, and printing parameters [4,8]. Furthermore, additive manufacturing and layer-by-layer fabrication create microscopic irregularities and increased surface roughness, which may facilitate microorganism colonization [9,13]. To address these limitations, various post-processing strategies and surface treatments have been explored [14].

Light-activated glaze coatings have been suggested as an efficient approach to modify the surface of 3D-printed resins, offering uniform surface refinement—even in anatomically complex areas—while reducing roughness and improving wettability, color stability, and surface hardness [15–17]. Beyond surface characteristics, applying a glaze layer may also influence the mechanical behavior of the underlying printed substrate. However, available studies have primarily focused on surface properties, and the effect of different glazing materials on the flexural properties of 3D-printed denture resins has not yet been fully elucidated [15,18].

In addition to mechanical performance, the long-term clinical durability of glazed restorations depends on the structural integrity of the glaze-resin interface [19]. In aqueous functional environments, deterioration of this bond can result in cracking and partial delamination of the glaze layer, negating the initial surface benefits [19,20]. Differences in the mechanical and physicochemical properties between the coating material and the resin substrate—including the presence of inorganic SiO_2 nanoparticle fillers within certain commercial glaze materials or the application of the unpolymerized denture base resin itself as a coating—may influence interfacial stability and resistance to delamination over time [21–23].

Despite growing interest in surface coating (glazing), there is limited data directly comparing unfilled versus SiO_2 nanoparticle-containing commercial glaze materials [24,25]. The application of the unpolymerized denture base resin as a coating remains largely unexplored, although it could offer chemical compatibility and cohesive bonding during post-curing compared to commercial alternatives [23]. Similarly, the potential impact of different application protocols-such as whether a double-layer application seals surface defects more effectively compared to a single-layer- has not been elucidated.

This study aimed to evaluate: 1. the effect of different surface-coating materials—including nanoparticle-containing glaze materials, an unfilled glaze material, and the unpolymerized resin—applied in single and double layers on the flexural properties of a 3D-printed denture base resin, and 2. the morphological integrity and delamination risk at the coating-resin interface following long-term water storage. The null hypotheses were that 1. surface-coating material would have no significant effect on flexural strength or flexural modulus, 2. the number of coating layers would have no significant effect on these properties, and 3. surface-coating material would not influence post-storage surface morphology.

2. Materials and Methods

2.1. Specimen Preparation

All specimens were fabricated using a stereolithography (SLA) 3D printer (Form 3B+; Formlabs Inc., Somerville, MA, USA) with a commercially available denture base resin (Denture Base Resin, shade OP; Formlabs Inc., Somerville, MA, USA). Digital designs were generated as STL files using a computer-aided design (CAD) software program (exocad DentalCAD version 3.3 Chemnitz; exocad GmbH; Darmstadt, Germany) and processed in a 3D print preparation software (PreForm version 3.56.0; Formlabs Inc., Somerville, MA, USA) to optimize build orientation, layout, and support placement. Specimens were printed at a layer thickness of 50 µm at a 45-degree orientation relative to the build platform.

Quality control was performed on all specimens following printing. Dimensional accuracy was verified using a digital caliper to ensure adherence to specified target dimensions within a tolerance of ±0.1 mm. Additionally, specimens underwent visual inspection under an optical microscope to identify and exclude specimens exhibiting surface irregularities or voids prior to testing.

2.2. Surface Treatment

Following fabrication, specimens were washed with 99.9% high-purity isopropyl alcohol (Form Wash; Formlabs Inc., Somerville, MA, USA) and post-cured for 30 min at 80 °C submerged in glycerin (Form Cure; Formlabs Inc., Somerville, MA, USA) according to the manufacturer's instructions for the specific resin to prevent oxygen inhibition. While the manufacturer's instructions for the specific resin recommend two 30-min exposures with turning, this protocol was adapted to a single 30-min cycle due to the flat, standardized geometry of the experimental specimens, as opposed to complex, bulky denture bases. Prior to surface coating, one designated surface per specimen was conditioned via airborne-particle abrasion (MicroEtcher IIA; Zest Dental Solutions, Carlsbad, CA, USA) using 50 µm aluminum oxide (Al_2O_3) powder at a 90-degree nozzle angle, 10 mm distance, for 10 s at 2 bar (0.2 MPa) pressure, whereas the control group received no surface treatment.

Study specimens were categorized into 11 groups, including the untreated control group. The 10 surface-coated groups were based on five coating materials: four commercially available glaze materials—Palaseal (Kulzer GmbH, Hanau, Germany), NanoVarnish (Dreve Dentamid GmbH, Unna, Germany), VITA Akzent LC (VITA Zahnfabrik, Bad Säckingen, Germany), and Optiglaze Color Clear (GC Corporation, Tokyo, Japan)—and the unpolymerized denture base resin (Denture Base Resin, shade OP; Formlabs Inc., Somerville, MA, USA). Five groups received a single layer, while the remaining five groups received a double layer. To assess flexural strength and modulus, ten specimens per group (65 × 10 × 3.3 mm) were fabricated, whereas for surface integrity evaluation, one specimen per group (10 × 10 × 2 mm) was prepared.

The surface-coating materials were applied uniformly using a small, fine-tipped brush held parallel to the specimen surface to minimize air entrapment. Following application, the materials remained on the specimen surface for 30 s, prior to photo-polymerization. Light-curing was subsequently carried out using an LED unit (Bluephase G2, Ivoclar Vivadent AG, Schaan, Liechtenstein) in "High" mode and approximately 1 mm from the surface, according to the manufacturer's instructions. The exposure duration for each applied layer was 80 s for the VITA Akzent LC, Optiglaze Color Clear, NanoVarnish, and unpolymerized resin groups, and 90 s for the Palaseal group, to ensure adequate polymerization. Because the length of the flexural specimens exceeded the diameter of the curing light tip, polymerization was performed using multiple overlapping irradiation zones to ensure uniform coverage across the entire surface. For the surface integrity specimens, a single centered exposure was applied. For the double-layer groups, the second layer was applied 30 min after photo-

polymerization of the initial layer to establish a standardized procedure and allow for a sufficient post-polymerization period, and cured under the same conditions.

With regard to unpolymerized resin groups, an additional post-curing cycle was performed in the Form Cure unit immediately after light-curing. The coated specimens were placed directly on the unit's turntable without glycerin, with the coated surface facing upwards for 30 min at 80 °C. For the double-layer group (RII), the second layer was applied and cured using the same protocol. Thus, the cumulative Form Cure exposures reached 60 and 90 min for groups RI and RII, respectively.

The chemical composition of the surface-coating materials, along with the corresponding group codes, is summarized in Table 1, based on the respective Safety Data Sheets (SDS) and manufacturer technical documentation.

Table 1. Group codes and chemical composition of the surface-coating materials used in the study.

Group ID Code	Surface-Coating Material	LOT Number	Main Organic Matrix	SiO_2 Nanoparticles (wt%)	Cross-Linking Agents and Key Additives
C	None (control group)	-	-	-	-
RI, RII	Formlabs Denture Base Resin	BF24F10O	Methacrylate monomer (40–60%), UDMA (30–50%), PTT (5–10%)	-	Diphenyl(2,4,6-trimethylbenzoyl)phosphine oxide (<3%)
PI, PII	Palaseal	N010182	MMA (25–50%), triethylene triacrylate derivative (25–50%), BADGE-DA (5–10%)	-	Glycerol propoxylated acrylates (5–10%), polysiloxane hexa-acrylate (0–5%), phosphine oxide (1–4%)
NI, NII	NanoVarnish	506011X0	MMA, propan-2-ol, pentaerythritol acrylates	3–6	Diphenyl(2,4,6-trimethylbenzoyl)phosphine oxide (2.5–10%)
VI, VII	VITA Akzent LC	215160	MMA, HDI-acrylate oligomer, dimethacrylates	8–11	Pentaerythritol acrylates, other multifunctional acrylates
OI, OII	Optiglaze Color Clear	2504151	MMA	5–10	TiO_2 (2.5–5%), diphenyl(2,4,6-trimethylbenzoyl)phosphine oxide (1–2.5%)

I: single layer of surface-coating application; II: double layer of surface-coating application.

2.3. 3-Point Bending Tests

Mechanical performance was evaluated using an Electroforce 3550 testing system (TA Instruments, New Castle, DE, USA) with 15 kN capacity and dual synchronized linear motors. Flexural properties (modulus E_f and strength σ_f) were assessed utilizing an ISO 20795-1-based experimental design. Specimens were stored in deionized water at 37 °C for 7 days prior to testing, in polymeric containers, with all specimens from the same group immersed in 25 mL of deionized water per container. The extended storage period

(compared to the 50 h specified by ISO 20795-1) was chosen to better simulate initial clinical water sorption. Except for the control group specimens, the coating material was applied to the abraded surface of each specimen that contacted the supporting jigs during testing, as this surface is subjected to maximum tensile stress where crack propagation occurs. The width and thickness of each specimen were also measured using a digital caliper prior to mechanical testing (post-coating and final polymerization). Immediately before evaluation, specimens were wiped with a microfiber cloth, gently air-dried, and tested in ambient room conditions (23 ± 2 °C). Mechanical testing was conducted at a crosshead speed of 5 mm/min. The properties were calculated using Equations (1) and (2):

$$E_f = (L^3 m)/(4bd^3) \quad (1)$$

$$\sigma_f = (3FL)/(2bd^2) \quad (2)$$

where m is the slope of the linear elastic region (N/mm), b is the width, d is the thickness, F is the fracture load (N), and L represents the support span, which was set at 50 mm.

2.4. Surface Morphology and Elemental Analysis (SEM-EDS) After Water Immersion

The specimens were stored in separate polymeric containers, each containing 10 mL of deionized water, at 37 °C for 90 days. This specific period was selected based on previous literature [19,20] suggesting that coating degradation typically manifests after three months of functional use. The deionized water was replaced on a weekly basis. Topography and elemental composition were qualitatively analyzed using a JEOL JSM-7610F Plus SEM (JEOL Ltd., Tokyo, Japan) integrated with an Oxford AZTEC ENERGY ADVANCED X-act energy-dispersive spectroscopy (EDS) system (Oxford Instruments, Abingdon, UK). Prior to scanning electron microscopy (SEM) evaluation, the specimens were sputter-coated with carbon. Analysis was performed on the coated surface of each specimen at 15 kV accelerating voltage, 10–15 mm working distance, and magnifications of ×100, ×200, and ×1000. Due to the polymeric nature of the specimens, the thin profile of the coatings and the carbon sputter-coating procedure, EDS was utilized for qualitative elemental identification rather than absolute quantification.

2.5. Statistical Analysis

Analysis was performed using SPSS version 28 (IBM Corp., Armonk, NY, USA) with a significance level of $p < 0.05$. Data normality was verified via the Shapiro–Wilk criterion. Differences between single- and double-layer groups were assessed using independent t-tests or Mann–Whitney tests, as appropriate. Comparisons between the control and experimental groups were evaluated using one-way ANOVA with Tukey's post hoc analysis (when variances were homogeneous, as verified by Levene's test), or the Kruskal–Wallis test using Dunn's post hoc pairwise comparisons with a Bonferroni correction (when homogeneity of variances was violated).

3. Results

3.1. Flexural Properties

3.1.1. Descriptive Statistics

The Shapiro–Wilk test showed that the data for both flexural properties were consistent with a normal distribution across the study groups. Descriptive statistics (mean, standard deviation, median, and interquartile range) for flexural strength and flexural modulus are presented in Table 2. Group NII exhibited the lowest mean and median flexural strength values, whereas the highest were recorded in the C and RII groups. Regarding flexural

modulus, the lowest mean values were observed in Groups PII, VI, and VII, while Groups RI and RII demonstrated the highest mean and median values.

Table 2. Mean (SD) and median (IQR) flexural strength (in MPa) and modulus (in GPa) values of study groups.

	Flexural Strength in MPa		Flexural Modulus in GPa	
Study Group	**Mean (SD)**	**Median (IQR)**	**Mean (SD)**	**Median (IQR)**
C	68.58 (29.19)	68.35 (53.47)	1.96 (0.59)	2.16 (0.73)
RI	64.60 (14.25)	65.31 (23.81)	2.52 (0.12)	2.55 (0.26)
RII	66.08 (15.56)	68.13 (33.83)	2.57 (0.14)	2.58 (0.25)
PI	42.10 (12.54)	41.23 (17.70)	1.83 (0.38)	1.89 (0.63)
PII	38.64 (8.53)	36.77 (11.45)	1.67 (0.32)	1.67 (0.60)
NI	33.33 (11.27)	32.02 (14.61)	1.85 (0.48)	2.02 (0.95)
NII	27.96 (8.50)	25.36 (15.68)	1.73 (0.38)	1.78 (0.68)
VI	34.24 (14.57)	32.39 (30.73)	1.66 (0.52)	1.55 (0.90)
VII	36.43 (13.92)	36.82 (22.77)	1.67 (0.40)	1.55 (0.72)
OI	35.89 (10.92)	36.57 (17.95)	1.74 (0.35)	1.67 (0.35)
OII	37.83 (20.66)	31.30 (23.05)	1.77 (0.43)	1.96 (0.71)

C: Control, R: Unpolymerized resin, P: Palaseal, N: NanoVarnish, V: VITA Akzent LC, O: Optiglaze, I: single layer, II: double layer.

3.1.2. Comparison Among Single-Layer Versus Double-Layer Groups

The independent *t*-test showed that there were no statistically significant differences between the flexural strength values of single and double layer of all tested surface-coating material groups (RI-RII: $(t(18) = 0.223, p = 0.826)$; PI-PII $(t(18) = 0.721, p = 0.480)$; NI-NII $(t(18) = 1.205, p = 0.244)$; VI-VII $(t(18) = 0.343, p = 0.735)$; and OI-OII $(t(18) = 0.262, p = 0.796)$). The same statistical test also revealed no statistically significant differences between the flexural modulus values of the corresponding single and double-layer study groups (RI-RII: $t(18) = 0.822, p = 0.422$; PI-PII: $t(18) = 1.006, p = 0.328$; NI-NII: $t(18) = 0.593, p = 0.561$; VI-VII: $t(18) = 0.019, p = 0.985$; OI-OII: $t(18) = 0.142, p = 0.888$)).

3.1.3. Comparison Among the Control and Single-Layer Groups

As illustrated in Figure 1a, flexural strength distributions differed significantly across the groups according to the Kruskal–Wallis test $(X^2(5) = 25.431, p < 0.001)$. The Kruskal–Wallis test was used to examine whether the mean ranks of flexural strength values differ across groups and was applied because the assumption of homogeneity of variances was not met $(F(5,54) = 4.139, p = 0.003)$. Dunn's post hoc test with Bonferroni correction showed a significant difference between C and NI groups, C and VI groups, RI and NI groups, RI and VI groups and RI and OI groups (adjusted $p = 0.022, 0.035, 0.004, 0.007, 0.019$). It should be noted that the mean ranks, median values, and mean values of the C group were higher than those for the NI and VI groups, and also the mean ranks, median values, and mean values of the RI group were higher than those for the NI, VI and OI groups.

The assumption of homogeneity of variances for the flexural modulus values among study groups was not met $(F(5,54) = 3.280, p = 0.012)$. According to the Kruskal–Wallis test $(X^2(5) = 23.442, p < 0.001)$, the flexural modulus distributions differed significantly among study groups. Dunn's post hoc test with Bonferroni correction showed a significant difference between RI and PI groups, RI and NI groups RI and VI groups and RI and OI

groups (adjusted $p = 0.004$, 0.010, 0.001, and 0.001, respectively) (Figure 1b). Group RI has higher mean ranks, median values, and mean values than groups PI, NI, VI, and OI. No statistically significant difference in flexural modulus was detected between the C and RI groups (adjusted $p = 0.099$), despite the higher mean ranks, median values, and mean values recorded for the latter.

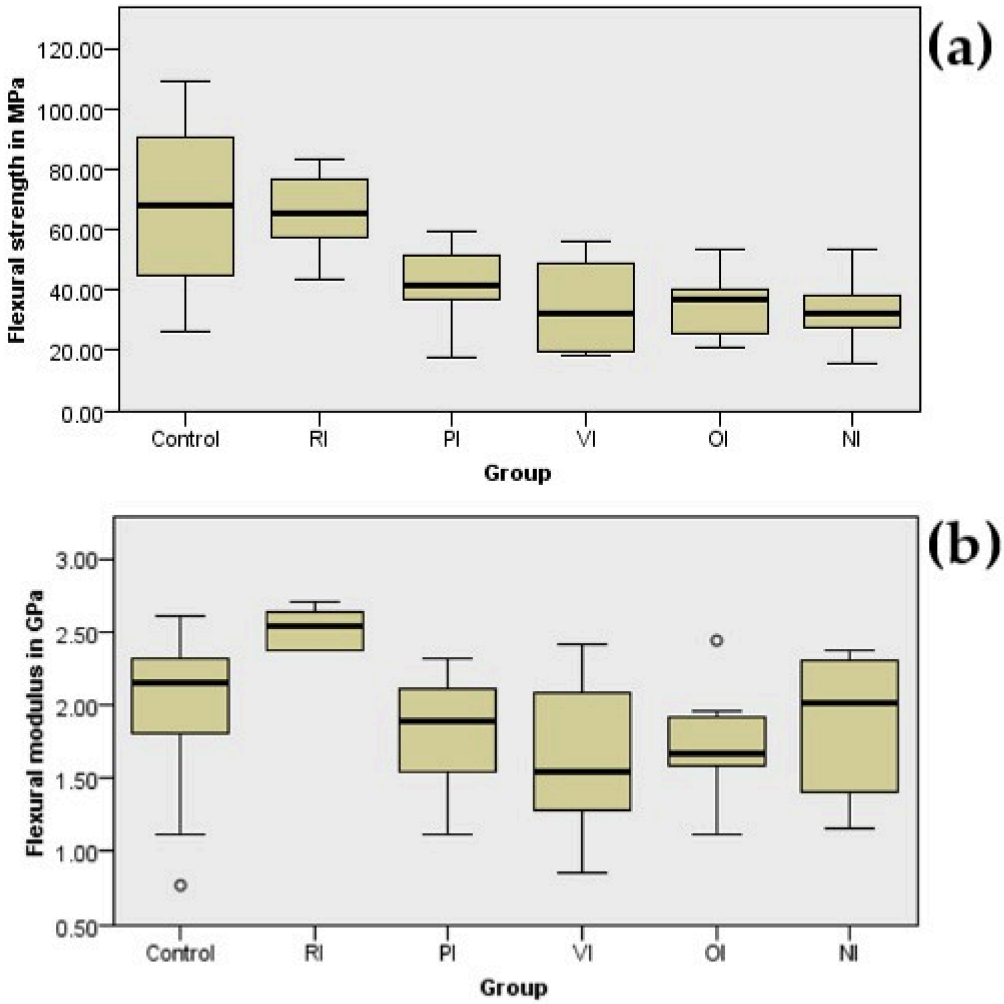

Figure 1. Comparison of (**a**) flexural strength (in MPa) and (**b**) flexural modulus (in GPa) among the control and single-layer application groups (RI, PI, VI, OI, NI). Horizontal lines inside the boxes represent medians, boxes indicate interquartile ranges, whiskers extend to minimum and maximum values, and open circles denote outliers.

3.1.4. Comparison Among the Control and Double-Layer Groups

A statistically significant difference in flexural strength distributions was identified among the control group and the double-layer surface-coating groups using the Kruskal–Wallis test ($X^2(5) = 26.353$, $p < 0.001$) (Figure 2a). Kruskal–Wallis test was applied because the assumption of homogeneity of variances did not hold, and because we are interested in determining whether the mean ranks of flexural strength differ across the groups. Dunn's post hoc test with Bonferroni correction showed a significant difference between C and NII groups, the RII and NII groups and the RII and OII groups (adjusted $p = 0.003$, <0.001, 0.041). It should be noted that group C has higher mean ranks, median values, and mean values than group NII, and group RII has higher mean ranks, median values, and mean values than groups NII and OII.

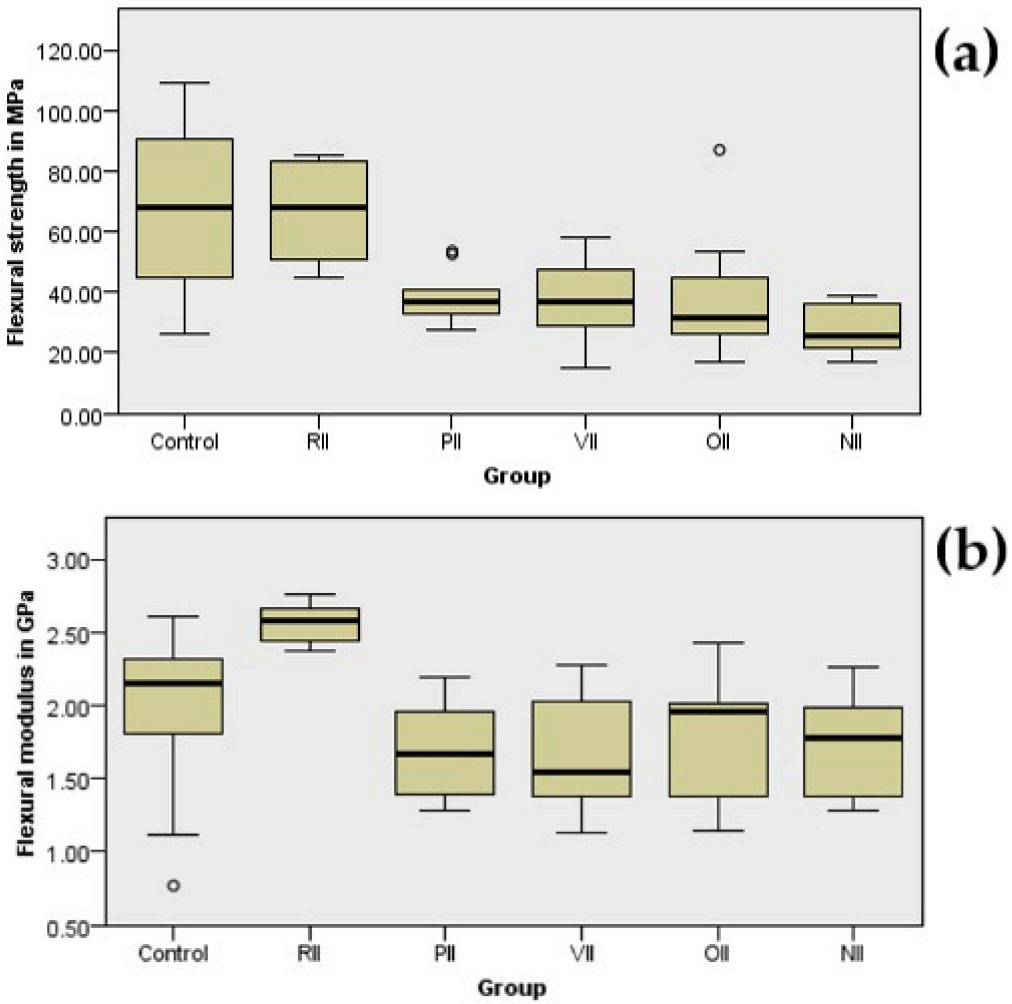

Figure 2. Comparison of (**a**) flexural strength (in MPa) and (**b**) flexural modulus (in GPa) among the control and double-layer application groups (RII, PII, VII, OII, NII). Horizontal lines inside the boxes represent medians, boxes indicate interquartile ranges, whiskers extend to minimum and maximum values, and open circles denote outliers.

Regarding the flexural modulus values among groups under study, the assumption of homogeneity of variances was violated ($F(5,54) = 2.789$, $p = 0.026$). The Kruskal–Wallis test regarding the hypothesis that population distributions are identical across all groups revealed a statistically significant overall difference in flexural modulus ($X^2(5) = 25.217$, $p < 0.001$). Dunn's post hoc test with Bonferroni correction showed a significant difference between RII and PII groups, RII and NII groups, RII and VII groups and RII and VII groups (adjusted $p = 0.001, 0.001, 0.001, 0.004$) (Figure 2b). Moreover, Group RII has higher mean ranks, median values, and mean values than groups PII, NII, VII, and OII. Although the RII group also demonstrated greater flexural modulus mean ranks, median values, and mean values than the control, the difference remained statistically non-significant (adjusted $p = 0.130$).

3.2. SEM-EDS Analysis After Water Immersion

Figures 3–5 display representative SEM micrographs illustrating the surface morphology of the 3D-printed denture base resin groups at various magnifications (×100, ×200 and ×1000, respectively). The characteristic staircase effect resulting from layer deposition is clearly visible in the control group (Figures 3a and 4a). While both commercial and experimental glaze materials provided a smooth surface topography, round-shaped voids

were observed on the surfaces coated with glaze coatings lacking SiO_2 nanoparticles. The distribution of anomalies of irregular shape which could be interpreted as Si-rich agglomerates, is depicted in Figure 5f–k, where they tended to form agglomerates. Furthermore, the recorded EDS spectra of the nano-reinforced glazed surfaces (Figure 6a–f) confirmed the presence of silicon (Si) within the material matrix, with Groups VI and VII additionally exhibiting distinct peaks corresponding to calcium (Ca), chlorine (Cl), sodium (Na), aluminum (Al), and magnesium (Mg).

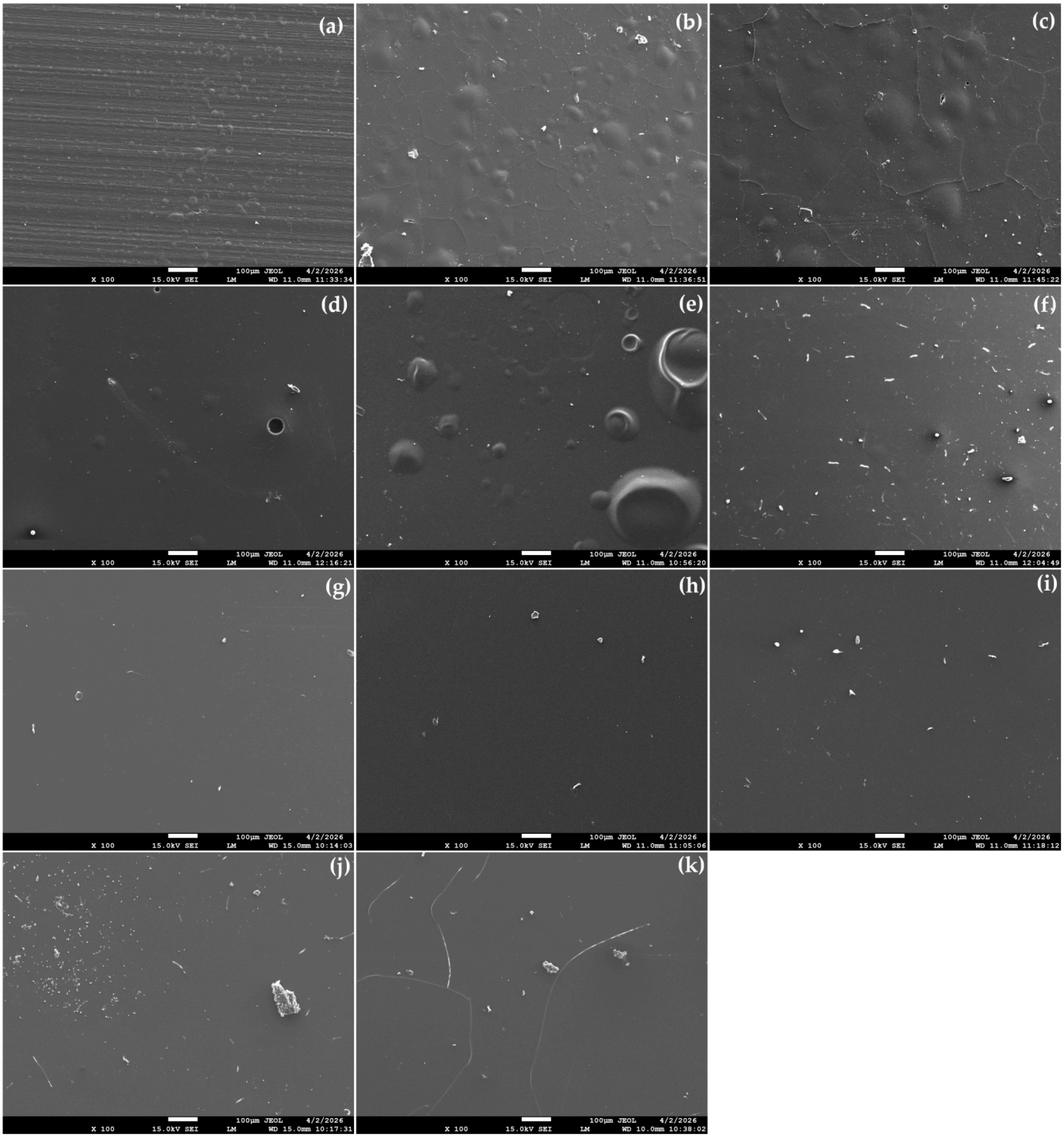

Figure 3. Representative SEM micrographs (×100 magnification, scale bar = 100 µm) illustrating the surface morphology of the tested groups: (**a**) Control, (**b**) RI, (**c**) RII, (**d**) PI, (**e**) PII, (**f**) NI, (**g**) NII, (**h**) VI, (**i**) VII, (**j**) OI, and (**k**) OII.

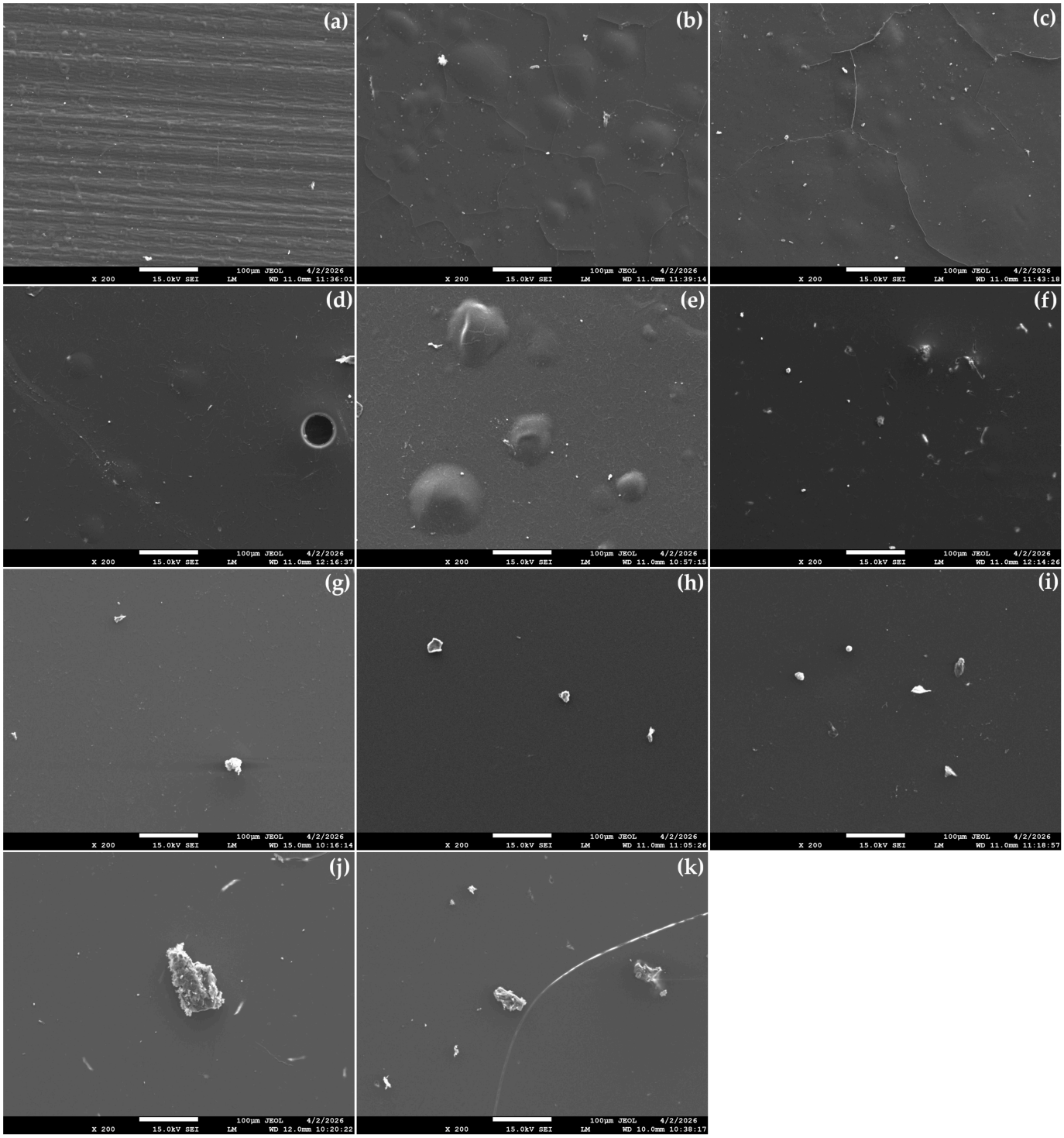

Figure 4. Representative SEM micrographs (×200 magnification, scale bar = 100 µm) illustrating the surface morphology of the tested groups: (**a**) Control, (**b**) RI, (**c**) RII, (**d**) PI, (**e**) PII, (**f**) NI, (**g**) NII, (**h**) VI, (**i**) VII, (**j**) OI, and (**k**) OII.

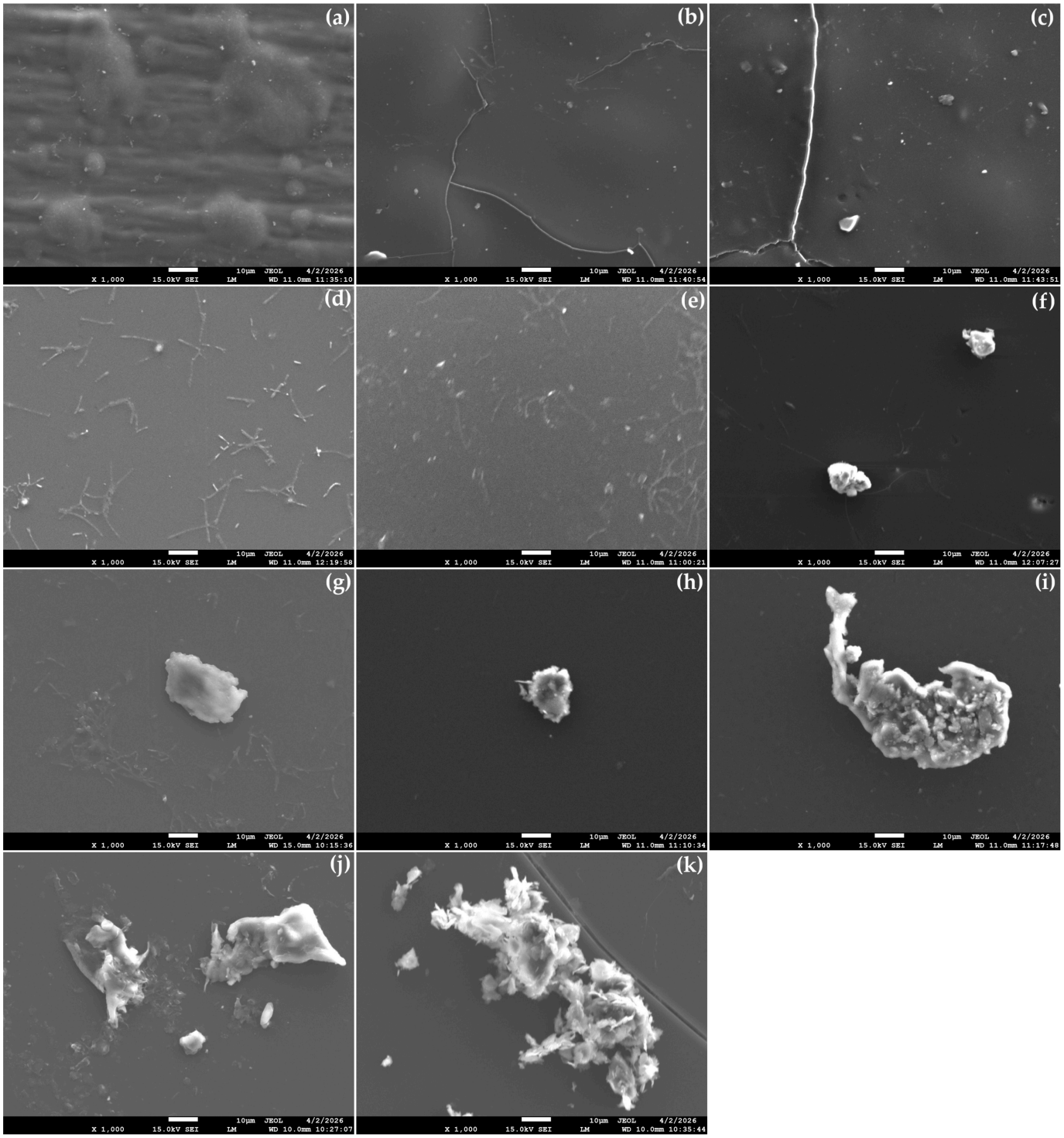

Figure 5. Representative SEM micrographs (×1000 magnification, scale bar = 10 μm) illustrating the surface morphology of the tested groups: (**a**) Control, (**b**) RI, (**c**) RII, (**d**) PI, (**e**) PII, (**f**) NI, (**g**) NII, (**h**) VI, (**i**) VII, (**j**) OI, and (**k**) OII.

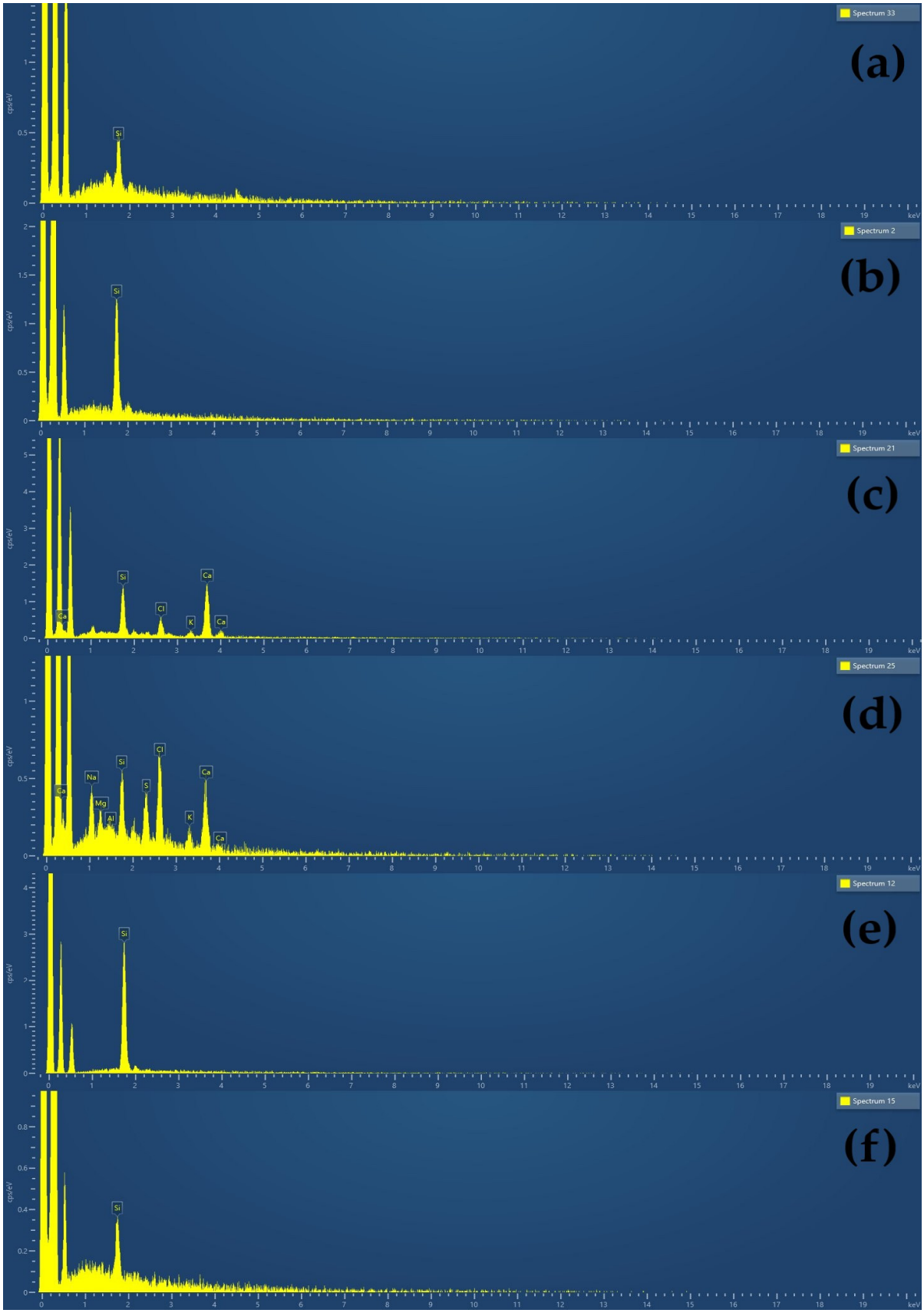

Figure 6. Representative EDS spectra indicating the elemental composition of the nano-reinforced surface-coating groups: (**a**) NI, (**b**) NII, (**c**) VI, (**d**) VII, (**e**) OI, and (**f**) OII. Prominent peaks correspond to the identified elements within each surface-coating matrix.

4. Discussion

The ISO standard 20795-1 for denture base polymers specifies a minimum flexural strength of 65 MPa. According to the results of the present study, the control group (untreated) specimens exhibited a mean flexural strength value slightly above this reference benchmark. The relatively high standard deviation observed in the control group may be related to SLA 3D-printing, where inherent micro-variations during layer-by-layer polymerization may influence the mechanical stability of specimens. This outcome aligns with previous literature reporting low flexural strength for 3D-printed resins [26,27], which occasionally falls below the ISO limit [15,28]. Notably, Coldea et al. (2025) reported flexural strength values of no more than 52.6 MPa, attributing this outcome to specimen storage conditions [29]. Indeed, storage in water has been shown to reduce the flexural strength of resins due to the plasticizing effect of water absorption [30,31]. Conversely, Izzettinoglu and Eroglu (2025), as well as Temizci and Bozoğulları (2024) [18,32], reported that the same 3D-printed resin material evaluated in the present study exhibited high flexural strength (median 93.2 MPa and mean 113.5 MPa, respectively) when specimens were polished and left unglazed. Both studies attribute this high performance mainly to the comprehensive post-curing protocols they applied.

Among the treated groups in this study, the specimens coated with the unpolymerized resin showed the highest flexural strength values, with mean values of 64.60 and 66.08 MPa for the single- and double-layer groups, respectively, performing closely to the 65 MPa benchmark. In contrast, all commercial coating groups exhibited substantially lower mean values. Thus, the commercial coating protocols were generally associated with lower flexural strength values, whereas application of unpolymerized resin largely preserved flexural strength relative to the untreated control. However, no statistically significant differences were observed in most pairwise comparisons between the control group and the surface-coating materials. The control group exhibited significantly higher flexural strength only when compared with the NanoVarnish (single and double layer) and VITA Akzent LC (single layer) groups. Similar results were reported in a previous study comparing the flexural strength of unglazed specimens to those coated with a methyl methacrylate (MMA)-based glaze [15]. The authors attributed this reduction to either the formation of a rigid surface layer by the coating, which limits the specimen's bending capacity, or the presence of methacrylate compounds in the glaze material, which may act as plasticizers, disrupting the intermolecular interactions of the polymer chains [15]. Another recent study evaluating the same 3D-printed base material (Formlabs Denture Base Resin) also reported a statistically significant reduction in flexural strength after surface coating with VITA Akzent LC, with values falling below the ISO threshold [18]. A clear trend appears to exist among the commercial coating materials, wherein their application leads to a reduction in flexural strength. However, the exact mechanisms underlying this effect cannot be hypothesized and require further investigation. It must be noted that comparisons between the control and surface-coating groups evaluate complete surface-treatment protocols; thus, the individual effects of coating application and airborne-particle abrasion cannot be independently assessed.

The flexural modulus results showed an analogous pattern regarding the effect of the surface-coating materials. The control group exhibited a mean flexural modulus of 1.96 GPa and a median of 2.16 GPa, indicating that the material does not fully meet the corresponding ISO requirement (2 GPa) under the 7-day water-storage conditions. Coldea et al. (2025) reported corresponding values of up to 1.84 GPa, which fall below this ISO threshold [29]. The groups coated with the unpolymerized resin (both single and double layers) presented the highest flexural modulus values. While their superiority was statisti-

cally significant compared to all commercial glaze materials, it did not differ significantly from the control specimens.

These findings suggest that surface-coating materials did not significantly enhance the flexural properties of the 3D-printed base resin; instead, commercial products in particular tend to impair them. Applying a single or double layer of surface-coating material did not result in a statistically significant difference in flexural strength or flexural modulus, regardless of the material used. Additionally, the incorporation of nanoparticles into their composition failed to improve their flexural performance under the conditions of the present study. Although it has been reported that TiO_2 and SiO_2 nanoparticles can improve the mechanical properties of denture base resins when incorporated into them [33–35], their presence within the coating material does not appear to possess this capacity. By merely sealing the resin surface, the polymerized coatings did not succeed in overcoming the inherent weaknesses of the 3D-printed resin. Factors influencing the synthesis and structure of the polymer network, along with post-polymerization processing conditions, may be more critical for the mechanical enhancement of 3D-printed dentures. Conversely, the application of the unpolymerized resin yielded the most favorable results, performing closely to the 65 MPa reference value. This positive outcome can be attributed to the chemical compatibility between the unpolymerized resin coating and the printed resin, which promotes a highly cohesive, monolithic bond during post-curing and avoids the elastic modulus mismatch that causes brittle commercial glaze materials to fracture prematurely under bending stress. Furthermore, the low viscosity of the unpolymerized resin allows it to flow easily into surface microporosities, stair-stepping print lines, and microcracks [16]. By sealing and "healing" these surface defects, the coating successfully eliminates critical stress-concentration points that would otherwise trigger crack propagation. Alternatively, the superior performance of the unpolymerized resin groups must be viewed in the context of their specific treatment protocol. Unlike the commercial glazes, this coating required an additional post-curing cycle in the Form Cure unit. This extended post-curing may have further increased the degree of conversion and cross-linking of the underlying printed substrate, enhancing its flexural properties independently of the coating material itself. These mechanisms, however, were not directly investigated in the present study and should therefore be considered hypothetical.

Scanning electron microscopy (SEM) analysis revealed that the surface-coating materials effectively eliminated the staircase effect inherent to the 3D printing process. However, after 90 days of water storage, SEM examination revealed spherical voids and surface irregularities in Palaseal- and unpolymerized resin-coated specimens, whereas the nanoparticle-containing commercial coatings showed a more continuous surface appearance. This effect cannot be attributed solely to the nanoparticle presence. Many factors such as compositional differences, variations in the organic matrix and cross-linking may affect the interfacial bond of the commercial coating formulations. These findings may indicate differences in coating integrity; however, because no baseline SEM examination or cross-sectional interfacial analysis was performed, the observations remain descriptive, and the observed defects cannot be conclusively attributed to water-induced surface debonding. Previous studies have reported similar outcomes. Specifically, Dayrell et al. (2011) evaluated Palaseal as a surface sealer to improve the bond between a soft liner and a conventional denture base resin, observing delamination after three months of storage [19]. The same surface-coating material, when applied to heat-cured dentures in a clinical study, developed cracks after three months of use, with the authors suggesting that delamination occurred due to the rigidity acquired by the surface-coating material after polymerization [20]. Similarly, another study evaluating a double-layer Optiglaze coating on 3D-printed denture base resins after aging for 14, 30, and 60 days in distilled water and other media reported glaze delamination from the resin

surface, which the authors attributed to a flexibility disparity between the coating and the 3D-printed substrate [22]. In the present study, however, the same material remained intact after three months of water storage. This discrepancy may be attributed to either the absence of artificial aging or the air abrasion protocol performed prior to coating. Air abrasion was executed in accordance with the manufacturers' instructions to increase surface roughness, thereby promoting mechanical interlocking between the base resin and the surface-coating material. Moreover, the overall effect of air abrasion on the mechanical properties of 3D-printed denture base resins remains controversial; indeed, some literature suggests that air abrasion can cause surface defects and microcracks, potentially leading to a deterioration in mechanical properties, including flexural strength [18].

The findings of this in vitro study cannot be directly translated into clinical recommendations. It can be inferred that the use of commercial glaze materials should be approached with caution, especially in denture bases expected to withstand high functional stresses, as their application may reduce flexural strength below acceptable limits. The application of unpolymerized denture base resin may present a reliable alternative for sealing surface defects without compromising mechanical integrity, an issue which merits further investigation.

A key strength of this study is its comprehensive evaluation and comparison of five different surface-coating materials—including both experimental and commercial systems, with or without nanoparticle reinforcement—on the flexural properties of 3D-printed denture base resins. Furthermore, these properties were evaluated utilizing a standardized experimental design based on the protocols specified by the relevant ISO standards, thereby enhancing reproducibility of the methodology, despite the intentionally extended water conditioning period. Additionally, to the authors' knowledge, the comparison between single- and double-layer glaze applications represents the first attempt to evaluate the impact of application protocol on the mechanical properties of 3D-printed denture base resins.

Several limitations must be acknowledged. The in vitro design of this study is a significant limitation, as storage in deionized water cannot fully replicate the complex oral environment, which includes pH fluctuations, salivary enzymes, and repetitive mechanical wear. The flexural specimens did not undergo artificial aging protocols (e.g., thermocycling). Furthermore, the evaluation was restricted to a single brand of SLA resin. The SEM-EDS analysis was conducted on a single specimen per group without baseline (pre-immersion) morphological evaluation. As this was intended as an exploratory qualitative evaluation, the morphological findings should be interpreted with caution. Future studies including baseline imaging may enable more reliable assessment of immersion-related changes. Finally, further research is warranted to thoroughly investigate other critical parameters essential to clinical success, such as surface roughness, coating thickness, wear resistance and microbial colonization.

5. Conclusions

Within the limitations of this in vitro study, the following conclusions can be drawn:

- The application of commercial glaze materials did not enhance the flexural properties of the 3D-printed denture base resin; instead, certain commercial products significantly reduced them.
- The untreated control group exhibited the highest mean flexural strength values. Among the treated groups, the specimens coated with the unpolymerized denture base resin (applied as either a single or double layer) maintained the highest values for both flexural strength and flexural modulus, remaining close to the corresponding ISO benchmarks.

- The number of applied glaze layers (single versus double) had no statistically significant impact on either the flexural strength or the flexural modulus of the 3D-printed denture base resin.
- All surface-coating materials successfully eliminated the printing staircase effect of the 3D printing process. Additionally, after three months of water storage, the commercial formulations containing nanoparticles showed no visible signs of localized debonding.

Author Contributions: Conceptualization, I.T. and E.K.; methodology, I.T., O.N., S.K., S.C. and E.K.; software, A.A., N.M. and S.C.; validation, A.A. and N.M.; formal analysis, I.T. and S.C.; investigation, I.T. and A.A.; resources, A.A. and N.M.; data curation, I.T. and S.C.; writing—original draft preparation, I.T.; writing—review and editing, O.N., S.K., S.C., A.A. and E.K.; visualization, I.T. and S.C.; supervision, E.K.; project administration, I.T. All authors have read and agreed to the published version of the manuscript.

Funding: This research received no external funding.

Institutional Review Board Statement: Not applicable.

Informed Consent Statement: Not applicable.

Data Availability Statement: The data presented in this study are available upon request.

Acknowledgments: The authors would like to acknowledge the Physical Metallurgy Laboratory, School of Mechanical Engineering, Aristotle University of Thessaloniki, Thessaloniki, Greece, as well as the Centre for Research & Development of Advanced Materials (CERDAM), Centre for Interdisciplinary Research and Innovation (CIRI), Thessaloniki, Greece, for granting access to their research infrastructure and laboratory facilities.

Conflicts of Interest: The authors declare no conflicts of interest.

Abbreviations

The following abbreviations are used in this manuscript:

3D	Three-dimensional
EDS	Energy-dispersive spectroscopy
SEM	Scanning electron microscopy
SLA	Stereolithography

References

1. Diaz-Arnold, A.M.; Vargas, M.A.; Shaull, K.L.; Laffoon, J.E.; Qian, F. Flexural and Fatigue Strengths of Denture Base Resin. *J. Prosthet. Dent.* **2008**, *100*, 47–51. [CrossRef] [PubMed]
2. Zidan, S.; Silikas, N.; Haider, J.; Alhotan, A.; Jahantigh, J.; Yates, J. Evaluation of Equivalent Flexural Strength for Complete Removable Dentures Made of Zirconia-Impregnated PMMA Nanocomposites. *Materials* **2020**, *13*, 2580. [CrossRef] [PubMed]
3. Alshali, S.; Basunbul, G.; Basunbul, A.; Giordano, R. Comparison of the Flexural Strength of Printed and Milled Denture Base Materials. *BMC Oral Health* **2024**, *24*, 929. [CrossRef] [PubMed]
4. Azab, A.; Abdelhady, W.A.; Elwakeel, E.; Ashraf, M.; Wally, R.; Soliman, A.; Mohamed, M.A.; Abozaid, D. Systematic Review and Meta Analysis of Mechanical Properties of 3D Printed Denture Bases Compared to Milled and Conventional Materials. *Sci. Rep.* **2025**, *15*, 29207. [CrossRef] [PubMed]
5. Aguirre, B.C.; Chen, J.H.; Kontogiorgos, E.D.; Murchison, D.F.; Nagy, W.W. Flexural Strength of Denture Base Acrylic Resins Processed by Conventional and CAD-CAM Methods. *J. Prosthet. Dent.* **2020**, *123*, 641–646. [CrossRef] [PubMed]
6. Alqutaibi, A.Y.; Baik, A.; Almuzaini, S.A.; Farghal, A.E.; Alnazzawi, A.A.; Borzangy, S.; Aboalrejal, A.N.; AbdElaziz, M.H.; Mahmoud, I.I.; Zafar, M.S. Polymeric Denture Base Materials: A Review. *Polymers* **2023**, *15*, 3258. [CrossRef] [PubMed]
7. Abduo, J.; Rasaie, V. Digital Workflows in Prosthodontics. *Aust. Dent. J.* **2025**, *70*, S146–S158. [CrossRef] [PubMed]
8. Alqarawi, F.K.; Gad, M.M. Tendency of Microbial Adhesion to Denture Base Resins: A Systematic Review. *Front. Oral Health* **2024**, *5*, 1375186. [CrossRef] [PubMed]
9. Anadioti, E.; Musharbash, L.; Blatz, M.B.; Papavasiliou, G.; Kamposiora, P. 3D Printed Complete Removable Dental Prostheses: A Narrative Review. *BMC Oral Health* **2020**, *20*, 343. [CrossRef] [PubMed]

10. Goodacre, B.J.; Goodacre, C.J. Additive Manufacturing for Complete Denture Fabrication: A Narrative Review. *J. Prosthodont.* **2022**, *31*, 47–51. [CrossRef] [PubMed]
11. Arzani, S.; Khorasani, E.; Mokhlesi, A.; Azadian, S.; Ghodsi, S.; Mosaddad, S.A. Do 3D-Printed and Milled Denture Bases Differ in Microbial Activity and Adhesion? A Systematic Review and Meta-Analysis. *Int. Dent. J.* **2025**, *75*, 100857. [CrossRef] [PubMed]
12. Chander, N.G.; Gopi, A. Trends and Future Perspectives of 3D Printing in Prosthodontics. *Med. J. Armed Forces India* **2024**, *80*, 399–403. [CrossRef] [PubMed]
13. Dimitrova, M.; Corsalini, M.; Kazakova, R.; Vlahova, A.; Chuchulska, B.; Barile, G.; Capodiferro, S.; Kazakov, S. Comparison between Conventional PMMA and 3D Printed Resins for Denture Bases: A Narrative Review. *J. Compos. Sci.* **2022**, *6*, 87. [CrossRef]
14. Hassanpour, M.; Narongdej, P.; Alterman, N.; Moghtadernejad, S.; Barjasteh, E. Effects of Post-Processing Parameters on 3D-Printed Dental Appliances: A Review. *Polymers* **2024**, *16*, 2795. [CrossRef] [PubMed]
15. Carneiro Pereira, A.L.; dos Santos Silva, J.P.; Grangeiro, M.T.V.; de Medeiros, A.K.B.; Bottino, M.A.; Barão, V.A.R.; da Fonte Porto Carreiro, A. 3D-Printed Denture Base Resins: Glazing as an Alternative to Improve Surface, Mechanical, and Microbiological Properties. *J. Prosthodont.* **2024**, 1–12. [CrossRef] [PubMed]
16. Sulaya, K.; Swapna, B.V.; Nayak, V.M. The Science of Printing and Polishing 3D Printed Dentures. *F1000Research* **2025**, *13*, 1266. [CrossRef] [PubMed]
17. Nam, N.E.; Hwangbo, N.K.; Kim, J.E. Effects of Surface Glazing on the Mechanical and Biological Properties of 3D Printed Permanent Dental Resin Materials. *J. Prosthodont. Res.* **2024**, *68*, 273–282. [CrossRef] [PubMed]
18. Izzettinoglu, E.; Eroglu, E. Evaluation of Mechanical Properties and Color Stability of 3D-Printed Denture Base Materials Following Two Surface Treatments. *BMC Oral Health* **2025**, *25*, 671. [CrossRef] [PubMed]
19. Dayrell, A.; Takahashi, J.; Valverde, G.; Consani, R.; Ambrosano, G.; Mesquita, M. Effect of Sealer Coating on Mechanical and Physical Properties of Permanent Soft Lining Materials. *Gerodontology* **2012**, *29*, e401–e407. [CrossRef] [PubMed]
20. Sesma, N.; Laganá, D.C.; Morimoto, S.; Gil, C. Effect of Denture Surface Glazing on Denture Plaque Formation. *Braz. Dent. J.* **2005**, *16*, 129–134. [CrossRef] [PubMed]
21. Choi, J.J.E.; Uy, C.E.; Ramani, R.S.; Waddell, J.N. Evaluation of Surface Roughness, Hardness and Elastic Modulus of Nanoparticle Containing Light-Polymerized Denture Glaze Materials. *J. Mech. Behav. Biomed. Mater.* **2020**, *103*, 103601. [CrossRef] [PubMed]
22. Raszewski, Z.; Chojnacka, K.; Mikulewicz, M. Effects of Surface Preparation Methods on the Color Stability of 3D-Printed Dental Restorations. *J. Funct. Biomater.* **2023**, *14*, 257. [CrossRef] [PubMed]
23. Fernandez, P.K.; Unkovskiy, A.; Benkendorff, V.; Klink, A.; Spintzyk, S. Surface Characteristics of Milled and 3D Printed Denture Base Materials Following Polishing and Coating: An in-Vitro Study. *Materials* **2020**, *13*, 3305. [CrossRef] [PubMed]
24. Azpiazu-Flores, F.X.; Elfana, A.; Yang, C.C.; Morton, D.; Lin, W.S. Effect of Artificial Aging and Different Surface Finishing Protocols on the Flexural Strength and Surface Hardness of a Photopolymer for Manufacturing Monolithic Polychromatic Complete Dentures Using PolyJet 3D Printing. *J. Prosthodont.* **2024**, 1–9. [CrossRef] [PubMed]
25. Pereira, A.L.C.; de Souza Oliveira, L.P.; de Medeiros, A.K.B.; Matias Bezerra, P.T.; Sinha, D.; Barão, V.A.R.; Carreiro, A.d.F.P. Effectiveness of Glaze in Reducing Color Change and Staining in Denture Bases and 3D-Printed Teeth: An in-Depth Colorimetric Analysis. *Digit. Dent. J.* **2026**, *3*, 100060. [CrossRef]
26. Fouda, S.M.; Gad, M.M.; Abualsaud, R.; Ellakany, P.; AlRumaih, H.S.; Khan, S.Q.; Akhtar, S.; al-Qarni, F.D.; Al-Harbi, F.A. Flexural Properties and Hardness of CAD-CAM Denture Base Materials. *J. Prosthodont.* **2023**, *32*, 318–324. [CrossRef] [PubMed]
27. Alzaid, M.; Altoraibily, F.; Al-Qarni, F.D.; Al-Thobity, A.M.; Akhtar, S.; Ali, S.; Al-Harbi, F.A.; Gad, M.M. The Effect of Salivary PH on the Flexural Strength and Surface Properties of CAD/CAM Denture Base Materials. *Eur. J. Dent.* **2023**, *17*, 234–241. [CrossRef] [PubMed]
28. Fouda, S.; Ji, W.; Gad, M.M.; AlGhamdi, M.A.; Rohr, N. Flexural Strength and Surface Properties of 3D-Printed Denture Base Resins—Effect of Build Angle, Layer Thickness and Aging. *Materials* **2025**, *18*, 913. [CrossRef] [PubMed]
29. Coldea, A.; Mayinger, F.; Meinen, J.; Hoffmann, M.; Stawarczyk, B. Mechanical Properties of 3D Printed Denture Base Polymers. *J. Prosthet. Dent.* **2025**, *133*, 1361.e1–1361.e8. [CrossRef] [PubMed]
30. Gad, M.M.; Fouda, S.M. Factors Affecting Flexural Strength of 3D-Printed Resins: A Systematic Review. *J. Prosthodont.* **2023**, *32*, 96–110. [CrossRef] [PubMed]
31. Altarazi, A.; Haider, J.; Alhotan, A.; Silikas, N.; Devlin, H. Assessing the Physical and Mechanical Properties of 3D Printed Acrylic Material for Denture Base Application. *Dent. Mater.* **2022**, *38*, 1841–1854. [CrossRef] [PubMed]
32. Temizci, T.; Bozoğulları, H.N. Effect of Thermal Cycling on the Flexural Strength of 3-D Printed, CAD/CAM Milled and Heat-Polymerized Denture Base Materials. *BMC Oral Health* **2024**, *24*, 357. [CrossRef] [PubMed]
33. Naji, S.A.; Behroozibakhsh, M.; Kashi, T.S.J.; Eslami, H.; Masaeli, R.; Mahgoli, H.; Tahriri, M.; Lahiji, M.G.; Rakhshan, V. Effects of Incorporation of 2.5 and 5 Wt% TiO_2 Nanotubes on Fracture Toughness, Flexural Strength, and Microhardness of Denture Base Poly Methyl Methacrylate (PMMA). *J. Adv. Prosthodont.* **2018**, *10*, 113–121. [CrossRef] [PubMed]

34. Karci, M.; Demir, N.; Yazman, S. Evaluation of Flexural Strength of Different Denture Base Materials Reinforced with Different Nanoparticles. *J. Prosthodont.* **2019**, *28*, 572–579. [CrossRef] [PubMed]
35. AlGhamdi, M.A.; Fouda, S.M.; Taymour, N.; Akhtar, S.; Khan, S.Q.; Ali, M.S.; Elakel, A.M.; Nassar, E.A.; Gad, M.M. Comparative Evaluation of TiO_2 Nanoparticle Addition and Postcuring Time on the Flexural Properties and Hardness of Additively Fabricated Denture Base Resins. *Nanomaterials* **2023**, *13*, 3061. [CrossRef] [PubMed]

Disclaimer/Publisher's Note: The statements, opinions and data contained in all publications are solely those of the individual author(s) and contributor(s) and not of MDPI and/or the editor(s). MDPI and/or the editor(s) disclaim responsibility for any injury to people or property resulting from any ideas, methods, instructions or products referred to in the content.